Chemical Identification of Single Atoms in Heterogeneous III–IV Chains on Si(100) Surface by Means of nc-AFM and DFT Calculations

Martin Setvín,*,†,‡ Pingo Mutombo,† Martin Ondráček,† Zsolt Majzik,† Martin Švec,† Vladimír Cháb,† Ivan Ošťádal,‡ Pavel Sobotík,‡ and Pavel Jelínek†

†Institute of Physics, Academy of Sciences of the Czech Republic, Cukrovarnická 10, 162 00, Prague, Czech Republic, and ‡Department of Surface and Plasma Science, Charles University, V Holešovičkách 2, 180 00, Prague, Czech Republic

ABSTRACT

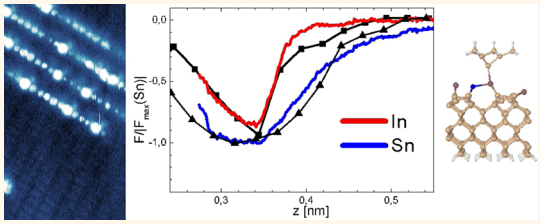

Chemical identification of individual atoms in mixed In–Sn chains grown on a Si(100)-(2 × 1) surface was investigated by means of room temperature dynamic noncontact AFM measurements and DFT calculations. We demonstrate that the chemical nature of each atom in the chain can be identified by means of measurements of the short-range forces acting between an AFM tip and the atom. On the basis of this method, we revealed incorporation of silicon atoms from the substrate into the metal chains. Analysis of the measured and calculated short-range forces indicates that even different chemical states of a single atom can be distinguished.

KEYWORDS: chemical identification · nc–AFM · Si(100) · chains · indium · tin

Scanning probe techniques (SPM), such as scanning tunneling microscopy (STM)[1] and atomic force microscopy (AFM)[2] are widely used to probe the atomic and electronic structure of surfaces and nanometer-sized objects. The most critical issues in interpretation of surface imaging are a reliable atomic resolution and the chemical identification. The latter still remains a challenge especially in complex nanostructures such as molecules, nanoparticles, or nanowires. STM and local spectroscopy of tunneling electrons (STS) show full complexity of the problem[3−5] but cannot accomplish the chemical resolution in general.

On the other hand, substantial advances in the chemical identification have been achieved by means of noncontact AFM (nc-AFM) in past few years. The method demonstrated its capability to resolve directly single chemical species on surfaces of semiconductors,[6] oxides,[7] and within organic molecules.[8,9] Most notably, it was shown[6] that the single-atom chemical identification can be achieved *via* site-specific force spectroscopy measurements[10] using frequency modulation atomic force microscopy (FM-AFM).[11]

In this case, the chemical identification was based on measuring properties of covalent bonds formed between an apex tip atom and a surface adatom. It was found that the magnitude of maximum attractive short-range (SR) force F_{max} is a characteristic quantity for each of the chemical species. Note that in this approach the dependence of the force spectra on a tip structure is overcome by a normalization procedure that consists in dividing the SR forces by a maximum SR attractive force in a given set of spectra (for detailed discussion see ref 6). The validity of such an approach was demonstrated on a semiconductor surface alloy composed of three isovalent species (Si, Sn, and Pb). In this particular case, the valence electrons of all surface atoms possess a very similar electronic structure close to the sp^3 hybridization with a characteristic dangling bond state close to the Fermi level. Despite the successful application of the method on the semiconductor surface alloy, its validity for more complex systems has not been fully established yet.

In this paper we demonstrate the strength of the method on a system of single–atom–wide chains on the Si(100)-(2 × 1)

* Address correspondence to setvin@fzu.cz.

Received for review May 6, 2012 and accepted July 2, 2012.

Published online July 02, 2012
10.1021/nn301996k

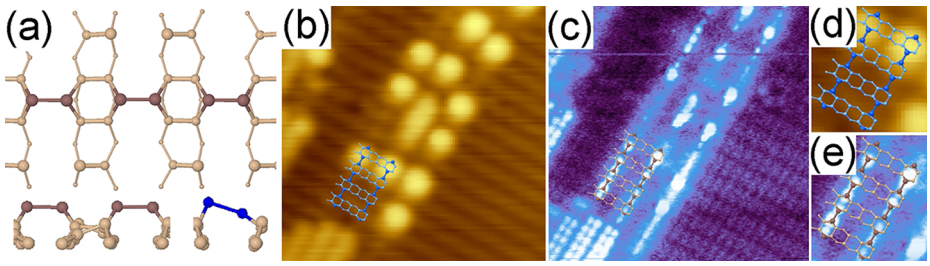

Figure 1. (a) Atomic structure of a chain on the Si(100)-(2 × 1) surface—top and side view. Red atoms denote indium which forms symmetric dimers. Blue color shows tin dimers with buckling. (b−e) Comparison of lateral resolution obtained by STM and nc-AFM. (b) STM image of the surface with three mixed InSn chains running from a step edge of the substrate (left bottom). $V_S = -2$ V. (c) The same area imaged by nc-AFM. Oscillation amplitude $A = 280$ pm, $f_0 = 73200$ Hz, quasiconstant height mode at $\langle \Delta f \rangle = -7$ Hz. (d,e) Details of the chains overlaid by atomic models. The models are also included in panels b and c to show the position of the magnified area.

surface, which consists of a random mix of group III and IV atoms. The mixing of two metals in atomically wide chains was investigated in the past[12−18] because of a possibility to tune the electronic structure of the chains. However, the fundamental problem in the research was chemical identification of single atoms in the observed structures, especially when different chemical species were arranged randomly in the chain. Recently, different structures were resolved in mixed InSn chains with a low Sn:In ratio and characterized using STM imaging, scanning tunneling spectroscopy, and DFT calculations.[19]

The Si(100)-(2 × 1) reconstruction[20] allows self-assembly of many different species into atomic chains (quantum wires[21]) due to a process called the surface polymerization reaction.[22] It is possible to grow chains composed of group III metals (Al, Ga, In, Tl),[23−28] group IV metals (Sn, Pb),[29,30] metals with a magnetic moment,[31] and many other metals[32] or even organic molecules.[33] The chains composed of the group III and group IV metals grow in a direction perpendicular to underlying Si dimer rows and they are composed of metal dimers oriented parallel to Si substrate dimers. A schematic model of In and Sn chains is depicted in Figure 1a. It is possible to mix III and IV group metals in the chain and retain the dimer structure.

In this paper we combine room-temperature (RT) FM-AFM measurements with DFT simulations to investigate the atomic and chemical structure of atomic chains composed of III and IV group metals grown on the Si(100) surface (see also ref 15). The chains are composed of randomly mixed homogeneous dimers (In−In and Sn−Sn) and heterogeneous dimers (In−Sn and others, as we will show in what follows). The chains with *a priori* unknown chemical structure, the presence of buckled dimers and atoms with different valences represent a challenging model for studying true atomic and chemical resolution by means of SPM. Despite that, we will demonstrate that the single-atom chemical identification within 1-D chains is still possible. Furthermore, we reveal an incorporation of individual silicon atoms into the heterogeneous metal chains, which has not been reported before and was not taken into account in interpretation of previous STM/STS measurements. We will also illustrate elementary processes occurring when the tip approaches to the metal dimers and the consequences for the atomic and chemical resolution. Finally we will discuss a possibility to resolve different chemical states of a single atom from the measured site-specific force spectra $F(z)$.

RESULTS AND DISCUSSION

The Atomic Resolution in FM-AFM. STM has been for a long time the most important method used for the investigation of 1-D metal chains on the Si(100) surface.[13−15] However, the lateral resolution achieved by STM is limited by surface electronic structure, which allows to resolve only the whole dimers, but not individual atoms. First we will compare the spatial resolution obtained by the STM and AFM techniques. Figure 1b,c shows STM and AFM images of an area of the Si(100) surface with three parallel mixed InSn chains running from an atomic step of the substrate. It is clearly seen that AFM provides much better lateral resolution—it is capable of imaging every single atom within the dimers. This observation has an important implication for both STM and AFM spectroscopic measurements—the site-specific force spectroscopy provides information with atomic spatial resolution, while scanning tunneling spectroscopy (STS) provides only information related to dimers.

Single-Atom Chemical Resolution. Both AFM and STM *images* themselves contain only very limited chemical information about the 1-D chains. The image contrast in FM-AFM[11] is obtained from a frequency shift Δf during lateral scanning. The Δf is related to the force acting between the tip and surface. But the relation between force $F(z)$ and the frequency shift $\Delta f(z)$ is rather complicated[34,35] as both short-range and long-range force components are present. To disentangle the force components, we perform the site-specific force spectroscopy above single atoms of the chain and a complementary measurement on a clean surface. The short-range force above each atom is obtained as a difference between these two $F(z)$ curves. Sugimoto *et al.*[6] found that the ratio between the maximum attractive short-range forces measured

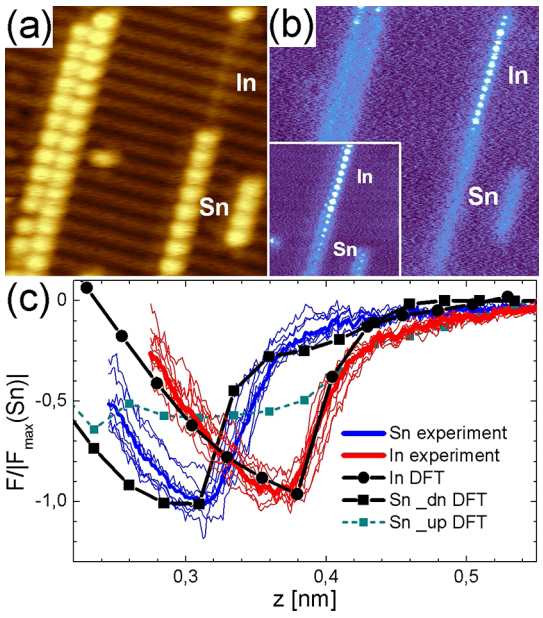

Figure 2. Force measurements above separate sections of In and Sn chains. (a) STM image, $V_S = -2$ V. Sections consisting of purely either of In or Sn atoms are marked. (b) AFM image of the same area at a tip−sample distance z = 0.39 nm. An inset shows the junction between In and Sn parts at a closer tip−sample distance z = 0.35 nm. (c) Force curves measured above In and Sn atoms. Experimental data are compared to DFT calculations. Sign convention: attractive forces are negative.

above two different chemical species was constant and independent of the tip apex. In particular, the ratios between maximum forces at the Si(111)-($\sqrt{3} \times \sqrt{3}$) mosaic were 0.77 for Sn:Si and 0.72 for In:Si. Accordingly the ratio between Sn and In can be estimated close to 1.07.

Separate Homogeneous In and Sn Chain Segments. Now we apply this approach[6] on separate homogeneous In and Sn chains. We prepared a structure that contained separate In and Sn chain sections where the atoms could not intermix (for details see the Experimental Details section). This can be achieved by a consecutive deposition of Sn and In atoms on the surface. In this case we can easily distinguish between the In and Sn segments by looking at filled-state STM images. Chains composed of group IV metals appear as bright lines in filled states while chains of group III metals are significantly less bright (see Figure 2a. The contrast in AFM images (Figure 2b) is opposite—indium sections are brighter than tin sections. The inset in Figure 2b shows that atomic resolution above the Sn section can be also obtained, but closer tip−sample distance is necessary. The different atomic contrast of In and Sn can be explained by different heights of the inspected In and Sn atoms above Si surface and by variation of the tip−sample interaction during the tip approach.[36]

Having sufficient lateral atomic resolution of atoms in 1−D chains, we performed the site-specific force spectroscopy above individual atoms of the 1−D chains. A typical set of measured $F(z)$ spectra is shown in Figure 2c. To eliminate the impact of the tip structure on the $F(z)$ dependence, we normalized the spectra by the overall maximum of the attractive force found in the set of measurements. We can clearly distinguish two different types of curves, unambiguously attributed either to In or Sn atoms. The ratio between the maximum attractive forces above In and Sn atoms is ∼1.06. This value is almost identical to the ratio obtained in the previous experiment on the Si(111) surface.[6] The two sets of the $F(z)$ spectra measured above In and Sn atoms show a perfect agreement with DFT calculations for homogeneous In and Sn chains (model structures in Figure 1a).

We note that the dimers in Sn chains consist of two nonequivalent Sn atoms − ″up″ and ″down″. Our experiments were conducted at RT, where thermal motion induces continual switching of up and down Sn atoms. What is more, it has been already shown that in FM-AFM a strong tip−sample interaction arises and affects the buckling direction of asymmetric dimers of the Si(100)-c(4 × 2) phase.[37] In our case, joint action of thermal motion and the proximity of the tip flips the Sn−Sn dimer buckling into the preferred down configuration under the tip. Consequently, we found excellent agreement between the $F(z)$ spectra measured above Sn atoms and dependences calculated for Sn atoms buckled down. This flipping mechanism is accompanied by the presence of pronounced dissipation signal,[38] which we actually observed in the experiment.

We conclude that In and Sn atoms forming homogeneous 1-D chains can be identified by means of the $F(z)$ spectroscopy despite the very similar values of the maximum attractive forces. The normalized $F(z)$ spectra show excellent agreement with DFT calculations.

Mixed InSn-Based Chains. Let us turn our attention to heterogeneous 1-D chains grown by simultaneous codeposition of Sn and In atoms now. Figure 3 shows a characteristic set of $F(z)$ force curves measured above a selected 1-D chain. Positions where individual $F(z)$ curves were acquired are marked in the inset. The measured force spectra can be divided to four groups with specific features: (i) Blue curves have a long-range "tail" reaching far from the surface. They correspond to brighter atoms in the AFM image in Figure 3. (ii) Red curves have a very similar maximum attractive force to the blue ones, but the force goes to zero more rapidly with increasing tip−sample distance. The dependence has a characteristic V-shape of the force maximum. (iii) Black curves have a significantly higher maximum attractive force than all other curves. (iv) The green curve has a similar shape to the red curves but the maximum attractive force is smaller. To get better insight into the origin of the F(z) spectra variation we performed DFT calculations simulating the probe interaction with different model structures of the chain.

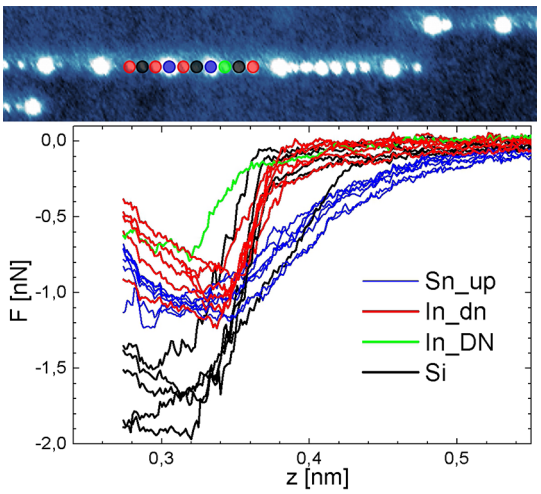

Figure 3. An example of short-range chemical forces measured above particular atoms of a mixed In−Sn chain. Different types of measured curves are distinguished by various colors. Positions corresponding to the measurements are marked by color circles in an AFM image detail. The chemical identification indicated in the plot is justified in the text.

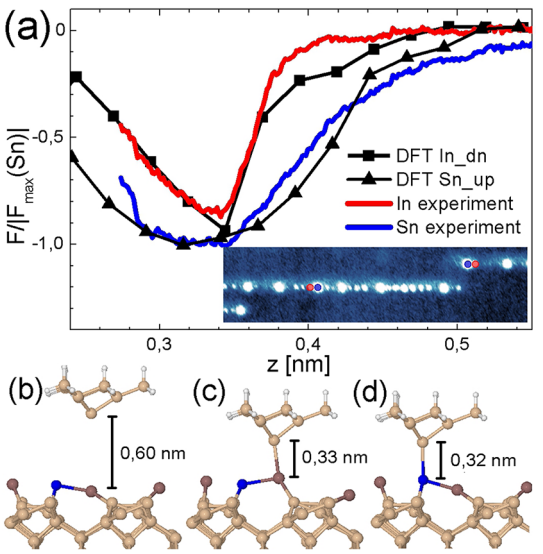

Figure 4. (a) Comparison between measured and calculated forces above an In−Sn heterodimer. (b) Calculated configuration where the tip is far from the dimer. (c) The tip above the In_dn atom at the maximum of attractive force. (d) The tip above the Sn_up atom at the maximum of attractive force.

A comparison between measured and calculated $F(z)$ spectra allows us to relate the four prototypical curves to particular chemical species.

In−Sn In−In Model Structure. The first model structure is a mixed In−Sn dimer inside an In chain, which is represented by a periodic In−Sn In−In structure in the calculation. It is known that mixed In−Sn dimers minimize their energy by buckling—the Sn atom is always buckled up and In down. According to the detailed analysis done by Magaud,[15] the Sn atom with four valence electrons prefers an sp^3 hybridization with one dangling bond perpendicular to a surface plane while the In atom with three valence electrons rehybridizes in a configuration close to sp^2 where all three bonds lie in one plane. Figure 4a shows calculated force curves above the Sn_up and In_dn atoms in the mixed dimer. The calculation is compared to force curves measured above In and Sn atoms in two dimers marked in the inset. The experimental data were averaged from eight measurements (four measurements for each marked atom).

The data calculated for Sn_up fits the blue curve. The Sn atom is initially buckled up and its vertical position does not change significantly during approaching the tip (see Figure 4b,d; the whole movie of the tip approaching is available as Supporting Information). The long-range "tail" of the Sn_up atom force seems to originate partially from the buckled up position and partially from additional electrostatic forces induced by charge transfers within the chain.[15] The red curve matches very well with data calculated for the In_dn atom located in the In−Sn dimer. The In atom is initially buckled down and the buckling is switched at a certain distance. It results in a sharp increase of the force and creates the characteristic "V"-shape of the force maximum. Even though the maximum attractive forces are very similar for In_dn and Sn_up, the chemical nature of the atoms can be recognized from characteristic features of the $F(z)$ dependence related to dimer buckling. The features were illustrated on the model structure, but they are general for any mixed configuration of In and Sn.

In−Sn Sn−In and In−Si Sn−In. An attractive force with a larger maximum (see black curves in Figure 3) was reproducibly measured above a configuration of heterogeneous dimers characterized as In−Sn Sn−In from STM images.[19] Such a structure was also predicted to be the most stable configuration in mixed InSn chains and is frequently encountered in grown mixed InSn chains. An example of a set of force spectra measured above individual atoms of this structure is in Figure 5. Further measurements with different tips are included in the Supporting Information.

We carried out a series of calculations of the $F(z)$ spectra above each atom in the In−Sn Sn−In model chain (see Figure 5b) in order to explain the measured curves. The blue, red, and green curves show excellent agreement with the DFT calculation for the In−Sn Sn−In sequence. According to the previous discussion, the atoms corresponding to the blue and red curves can be identified as Sn_up and In_dn atoms, respectively. The green curve is similar to an In_dn atom, though the maximum force is smaller. This feature and its origin will be discussed later. However, the black curve exhibiting the largest force is not reproduced. We tried possible configurations of In and Sn atoms in the chain, but the calculations clearly show that the large force cannot be reproduced in this way.

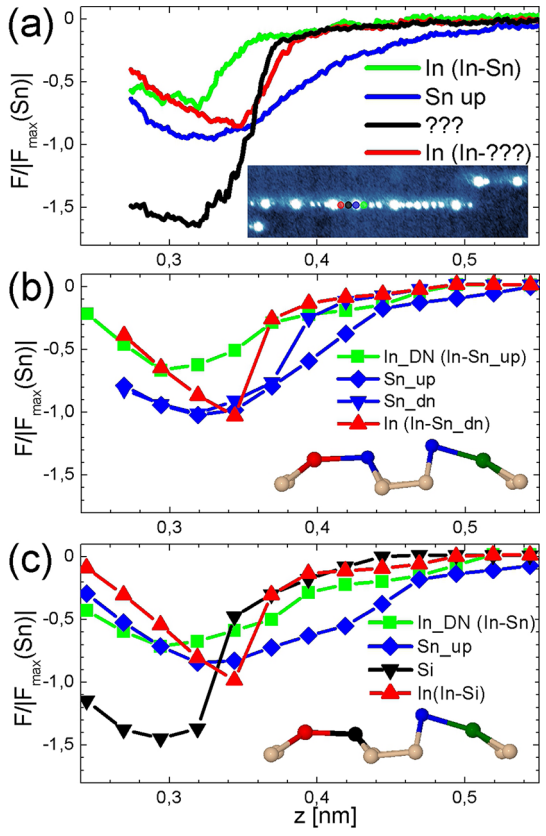

Figure 5. (a) A frequently encountered sequence of force curves measured above four neighboring atoms. (b) DFT calculation of force curves above atoms of the In−Sn Sn−In structure. (c) DFT calculation above the In−Sn Si−In structure.

Having a close look, one can notice that the experimental ratio between F_{max} of the black curve and the corresponding value for Sn is close to the Si:Sn ratio measured by Sugimoto *et al.*[6] It points to the possible presence of Si atoms in the chains, which has not been detected by STM/STS so far. It can be indeed expected that atoms from the substrate might be incorporated into growing chains because the presented mixed chains were prepared at 100−150 °C. (Note that the Si(100) surface covered by In undergoes a complex reconstruction at temperatures as low as 300 °C.[24])

To confirm this hypothesis, we substituted one Sn atom in our model by Si, creating an In−Sn Si−In sequence. The force curve calculated for the Si atom shows excellent agreement with the experimental data (see Figure 5c), so the black curves in Figure 3 can be attributed to Si atoms. The average ratio between the maximum forces above Si and Sn atoms is 1.49 in our measurements. In the previous study[6] on the Si(111) surface the ratio was 1.30. The average maximum forces from our measurements and calculations are summarized in Table 1 and values previously measured on the Si(111) surface[6] are included for comparison. We note that the normalized maximum force for Sn in Figure 5 is smaller than 1 because the normalization

TABLE 1. Measured and Calculated Ratios between Maximum Forces above In, Sn, and Si Atoms in Heterogeneous Chains on Si(100) and a Mosaic Structure on Si(111) Surface

	Sn:In	Si:Sn
chains separate, experiment	1.06	
chains separate, DFT	1.05	
chains mixed, experiment	1.10	1.49
chains mixed, DFT	1.06	1.34
Si(111) mosaic, experiment[6]	1.07	1.30
Si(111) mosaic, DFT[6]		1.22

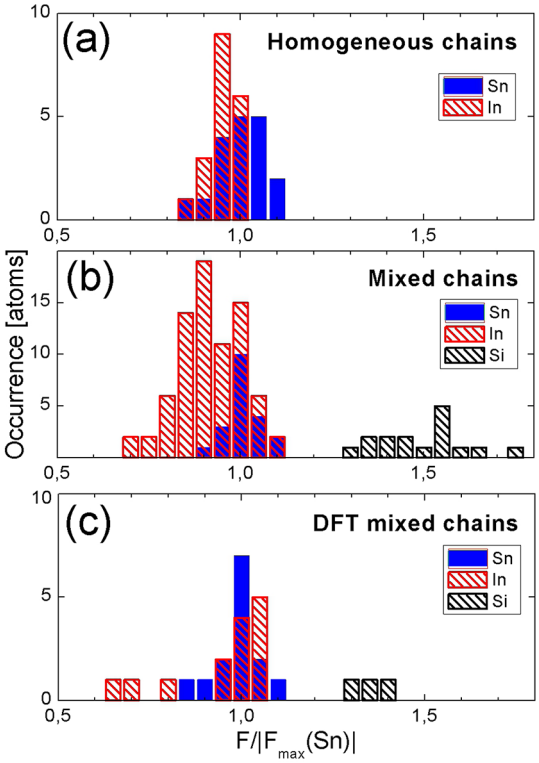

Figure 6. Histograms of maximum attractive forces measured above In, Sn atoms in homogeneous InSn chains (a); above In, Sn, and Si atoms in mixed chains (b); and calculated for different configurations of atoms in mixed chains (c).

uses the average F_{max}(Sn) from all DFT calculations performed. Dispersion of the calculated forces is shown in Figure 6c.

Dispersion of the Maximum Forces, Atomic and Electronic Configuration. We showed that the randomly mixed In, Sn, and Si atoms in the chains can be identified from the site-specific force spectra taken above individual atoms supported by DFT calculations. It brings a question why AFM provides a straightforward way for chemical identification while the same task is very complicated for STM. The weakness of STM originates from dimer buckling − each configuration of In, Sn and Si atoms relaxes to a unique buckled structure with a specific surface electronic structure.

The advantage of AFM is surprisingly in the strong tip−sample interaction. When the tip approaches close enough, a covalent bond between the tip and the investigated atom is formed, breaking the original atomic and electronic configuration. A precise analysis of our calculations shows that the maximum attractive force is attained for a very specific configuration of backbonds (each atom of the chain forms three bonds, called backbonds, with surrounding atoms—two pointing toward substrate Si atoms and one toward the other atom in the dimer). In most cases, according to our DFT calculations, the maximum force is reached when the investigated atom is buckled up and all three backbond angles are close to 90°. One angle is typically in a range from 75 to 90° and the two symmetric angles are from 90 to 100°.

Values of maximum attractive forces measured above particular atom types have interesting statistical properties. Figure 6 shows distributions of the normalized values measured above Sn, In, and Si atoms for three cases: (a) the homogeneous chain sections as shown in Figure 2; (b) data measured in the mixed chains; (c) values obtained by DFT calculations for various configurations of atoms. In the first case, the dispersions of histograms are small for In and Sn, which we attribute to the well-ordered structure of chains. In heterogeneous chains (Figure 6b), Sn atoms show even smaller dispersion than in the previous case. It originates from the fact that Sn always prefers the buckled up configuration in heterogeneous dimers. We can illustrate this on the example of our DFT calculations in Figure 5b. Both $F(z)$ curves taken above different Sn atoms in the In−Sn Sn−In structure become identical under attractive interaction with a probe. In other words, the attractive interaction between the tip and the sample exchanges buckling configuration of the two neighboring In−Sn dimers, that is, lower to upper and *vice versa*. Consequently, both Sn atoms reach the same configuration at a point of the maximum attractive force F_{max}, regardless of its original buckling orientation.

On the other hand, the dispersion for In atoms is significantly larger than in case of the homogeneous chains. We have already observed two different types of $F(z)$ curves (red and green in Figure 3), which we attributed, using the DFT simulations, to two slightly different buckling configurations of In atoms located in the adjacent heterogeneous dimers. Origin of the dispersion can be revealed from the DFT calculations

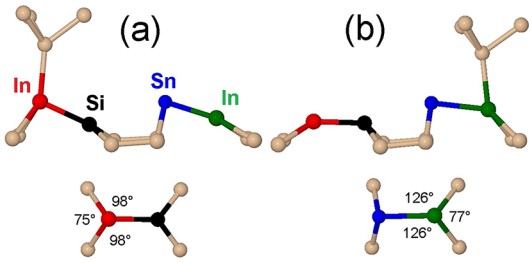

Figure 7. Configurations of the In−Sn Si−In structure at the maximum of chemical force. (a) Tip above the In atom in In−Si dimer, (b) tip above the In atom in In−Sn dimer. Side and top views of the system are shown and angles between backbonds are marked.

(see Figure 6c). The calculated maximum forces of In split into two distinct groups, one with a maximum force similar to the Sn, and the other group with the maximum force about 30% smaller. DFT calculations show that the smaller force is obtained for configurations where the tip does not switch the In atom up. An example of such case is the In−Sn Si−In structure in Figure 5. The In_DN atom in the In−Sn dimer is not switched by the approaching tip, while the other In atom (In−Si dimer) is switched. The configuration of the system at the maximum attractive force is in Figure 7. The whole movie of the tip approaching to the surface is in the Supporting Information.

The behavior of In atoms suggests that the force curves allow not only to identify single chemical species, but also to obtain information about the backbond configuration. In other words, we can distinguish different chemical states of a single atom.

CONCLUSION

Mixed In−Sn chains were investigated by means of nc-AFM and DFT calculations. We showed that the nc-AFM technique is capable of resolving individual atoms in dimers, providing much better lateral resolution than traditional STM. In addition, we demonstrated chemical resolution of single atoms by means of the force site spectra measurements above the particular atoms in the chains combined with advanced DFT calculations. On the basis of this approach, we were able to reveal the incorporation of Si atoms from the substrate into the chains during metal deposition at elevated temperature, which was not detected by previous STM studies. Finally, we discussed the possibility to distinguish different chemical states of a single atom from the force curves and DFT simulations.

EXPERIMENTAL DETAILS

All experiments were performed at room temperature on Omicron VT XA Q-plus AFM/STM machine in ultrahigh vacuum at pressures below 3×10^{-9} Pa. The measurements were done with a tuning fork based sensor with a separate connection for the tunneling current channel.[39] Typical characteristics of the sensor were as follows: resonant frequency f_0 = 73200 Hz, oscillation amplitude A = 0.3 nm, quality factor Q = 2000, spring constant k = 4300 N/m. A tungsten tip was attached to the tuning fork. The tip was cleaned by annealing at high

temperature and then it was treated on the Si(100) surface by application of voltage pulses. This procedure leads to picking clusters of silicon atoms from the substrate. All AFM measurements were done close to zero sample bias to minimize phantom forces induced by tunneling current.[40] Sb-doped Si(100) samples with a resistivity of 0.014 Ωcm were used. A procedure suggested in ref 41 was used to prepare a surface with low defect concentration.

The layer in Figure 2 was prepared by deposition of 0.04 ML of Sn at 100 °C followed by deposition of 0.04 ML of In at room temperature (RT). Finally 0.01 ML of Sn was deposited at RT to stabilize the In sections. All other presented layers of mixed In−Sn chains were prepared by codeposition of In and Sn. Sample temperature was kept at 100−150 °C during the deposition. The In:Sn ratio was strongly in favor of In (5:1 to 10:1) because such uneven concentrations allow partial characterization of the surface structures by means of STM[19] (*cf.* Figure 1b).

Presented AFM images were measured in a quasiconstant height mode. The tip−sample separation was kept constant by a weak feedback loop. The contrast in the image is obtained from the frequency shift Δf; all images were measured in the region of attractive short-range forces. This mode provided better lateral resolution than the constant Δf mode, and a risk of tip crashing was significantly lower.

Short range chemical forces were measured in the following way: $\Delta f(z)$ dependence was measured above an atom of the chain. Long range forces were determined by measuring the $\Delta f(z)$ dependence next to the chain. The two dependences were subtracted and the Sader formula[35] was used to convert the frequency shift to the force.

The absolute z-scale (*i.e.*, the nominal tip−sample distance) in the plots of experimental curves presented here was adjusted to fit the DFT results. Specifically, the measurement on the Sn atoms buckled-up was used as a reference to align the experimental and theoretical z-scales. All plotted forces are divided by an average force of an Sn atom buckled-up. The normalization is necessary because the absolute values of the force are not reproducible when measured by different tips, while the ratios between forces measured above different chemical species are tip-independent.[6] The measured force above an Sn atom ranged from 0.8 to 1.5 nN, depending on the tip apex. The calculated value was typically 2 nN.

Computational Details. We have performed DFT calculations within the local density approximation (LDA) as implemented in the Fireball code[42,43] in which a local atomic-orbital basis set and the MD-DFT (Molecular Dynamics based on the DFT) approach have been applied to determine the minimum total energy configuration. The optimized numerical local atomic orbitals were confined to regions limited by the corresponding cutoff radii. The Si cutoff radii were R_c(Si,s) = 4.8 au, R_c(Si,p) = 5.4 au, and R_c(Si,d) = 5.2 au. The In cutoff radii are R_c(In,s) = 5.2 au, R_c(In,p) = 6.0 au, and R_c(In,d) = 5.8 au. The Sn cutoff radii are R_c(Sn,s) = 5.2 au, R_c(Sn,p) = 5.7 au, and R_c(Sn,d) = 5.6 au. To simulate the Si(100) surface, we used a 4 × 6 unit cell made of 10 Si layers, the last one passivated by a bihydride layer. Both the bottom Si and the hydrogen atoms were kept fixed during the relaxation. The relaxation cycle was performed until the forces acting on free atoms and the difference in the total energy between two consecutive steps were below 0.05 eV/Å and 0.0001 eV, respectively. The InSn mixed dimers were placed in the troughs between the Si dimer rows. As for the AFM simulations, a Si(111) tip made of 10 atoms saturated by 15 H atoms at its base was used for force−distance calculations.[44] We initially placed the apex of the tip 6 Å above the surface. This distance was defined as the distance between the tip apex atom and the topmost surface atom. Then, we approached vertically the tip to the surface by a displacement step of 0.25 Å. During each step, the composite system was allowed to relax until the forces and the energy difference reached the criterion mentioned above. The short-range chemical force on the tip was determined during each step by summing the forces on all the fixed atoms.

Conflict of Interest: The authors declare no competing financial interest.

Acknowledgment. The work was supported by projects of GAČR P204/10/0952, GD202/09/H041 and GAAV IAA100100905. M.O. acknowledges the support by the Czech Science Foundation (GAČR) under the project P204/11/P578.

Supporting Information Available: Additional information and videos as described in the text. This material is available free of charge *via* the Internet at http://pubs.acs.org.

REFERENCES AND NOTES

1. Binnig, G.; Rohrer, H.; Gerber, C.; Weibel, E. Surface Studies by Scanning Tunneling Microscopy. *Phys. Rev. Lett.* **1982**, *49*, 57–61.
2. Binning, G.; Quate, C.; Gerber, C. Atomic Force Microscope. *Phys. Rev. Lett.* **1986**, *56*, 930–933.
3. Feenstra, R. M.; Stroscio, J. A.; Tersoff, J.; Fein, A. P. Atom-Selective Imaging of the GaAs(110) Surface. *Phys. Rev. Lett.* **1987**, *58*, 1192–1195.
4. Stipe, B. C.; Rezaei, M. A.; Ho, W. Single-Molecule Vibrational Spectroscopy and Microscopy. *Science* **1998**, *280*, 1732–1735.
5. Schmid, M.; Stadler, H.; Varga, P. Direct Observation of Surface Chemical Order by Scanning Tunneling Microscopy. *Phys. Rev. Lett.* **1993**, *70*, 1441–1444.
6. Sugimoto, Y.; Pou, P.; Abe, M.; Jelínek, P.; Perez, R.; Morita, S.; Custance, O. Chemical Identification of Individual Surface Atoms by Atomic Force Microscopy. *Nature* **2007**, *446*, 64–67.
7. Foster, A. S.; Barth, C.; Henry, C. R. Chemical Identification of Ions in Doped NaCl by Scanning Force Microscopy. *Phys. Rev. Lett.* **2009**, *102*, 256103.
8. Gross, L.; Mohn, F.; Moll, N.; Liljeroth, P.; Meyer, G. The Chemical Structure of a Molecule Resolved by Atomic Force Microscopy. *Science* **2009**, *325*, 1110–1114.
9. Gross, L.; Moll, N.; Meyer, G.; Ebel, R.; Abdel-Mageed, W. M.; Jaspars, M. Organic Structure Determination Using Atomic-Resolution Scanning Probe Microscopy. *Nature Chem.* **2010**, *2*, 821–825.
10. Lantz, M. A.; Hug, H. J.; Hoffmann, R.; van Schendel, P. J. A.; Kappenberger, P.; Martin, S.; Baratoff, A.; Guntherodt, H.-J. Quantitative Measurement of Short-Range Chemical Bonding Forces. *Science* **2001**, *291*, 2580–2583.
11. Albrecht, T. R.; Grutter, P.; Horne, D.; Rugar, D. Frequency Modulation Detection Using High-Q Cantilevers for Enhanced Force Microscope Sensitivity. *J. Appl. Phys.* **1991**, *69*, 668–673.
12. Nogami, J. Self-Assembled Single Atom Wide Metal Lines on Si(001) Surfaces. *Atom. Mol. Wires* **1997**, 11–21.
13. Juré, L.; Magaud, L.; Mallet, P.; Veuillen, J.-Y. Co-deposition on In and Sn on the Si(100) 2 × 1 Surface: Growth of a One-Dimensional Alloy? *Appl. Surf. Sci.* **2000**, *162−163*, 638–643.
14. Magaud, L.; Pasturel, A.; Jure, L.; Mallet, P.; Veuillen, J. Y. In, Sn Dimers on Si(100)2 × 1 Surface: *Ab Initio* Calculations and STM Experiments. *Surf. Sci.* **2000**, *454*, 489–493.
15. Magaud, L.; Pasturel, A.; Veuillen, J.-Y. Instability of Metallic In−Sn Dimer Lines on Si(100) 2 × 1 Surface. *Phys. Rev. B* **2002**, *65*, 245306.
16. Putungan, D. B.; Ramos, H. J.; Chuang, F. C.; Albao, M. A. Modeling of Co-deposition of Indium and Tin on Silicon-(100): A Kinetic Monte Carlo Study. *Int. J. Mod. Phys. B* **2011**, *25*, 1889–1898.
17. Bowler, D. R.; Bird, C. F.; Owen, J. H. G. 1D Semiconducting Atomic Chain of In and Bi on Si(001). *J. Phys.Condens. Matter* **2006**, *18*, L241–L249.
18. Owen, J. H. G.; Miki, K. Growth of Ag Nanoclusters on a 1D Template. *Surf. Sci.* **2006**, *600*, 2943–2953.
19. Sobotík, P. **2012**, to be published.
20. Uda, T.; Shigekawa, H.; Sugawara, Y.; Mizuno, S.; Tochihara, H.; Yamashita, Y.; Yoshinobu, J.; Nakatsuji, K.; Kawai, H.; Komori, F. Ground State of the Si(100) Surface Revisited—Is Seeing Believing? *Prog. Surf. Sci.* **2004**, *76*, 147–162.
21. Xia, Y.; Yang, P.; Sun, Y.; Wu, Y.; Mayers, B.; Gates, B.; Yin, Y.; Kim, F.; Yan, H. One-Dimensional Nanostructures: Synthesis,

Characterization, and Applications. *Adv. Mater.* **2003**, *15*, 353–389.
22. Brocks, G.; Kelly, P. J.; Car, R. Adsorption of Al on Si(100): A Surface Polymerization Reaction. *Phys. Rev. Lett.* **1993**, *70*, 2786–2789.
23. Nogami, J.; Park, S.-I.; Quate, C. F. Behavior of Ga on Si(100) as Studied by Scanning Tunnel Microscopy. *Appl. Phys. Lett.* **1988**, *53*, 2086–2088.
24. Nogami, J.; Baski, A. A.; Quate, C. F. Aluminum on the Si(100) Surface: Growth of the First Monolayer. *Phys. Rev. B* **1991**, *44*, 1415–1418.
25. Kotlyar, V. G.; Saranin, A. A.; Zotov, A. V.; Lifshits, V. G.; Kubo, O.; Ohnishi, H.; Katayama, M.; Oura, K. High-Temperature Interaction of Al with Si(100) Surface at Low Al Coverages. *Surf. Sci.* **2002**, *506*, 80–86.
26. Albao, M. A.; Evans, M. M. R.; Nogami, J.; Zorn, D.; Gordon, M. S.; Evans, J. W. Monotonically Decreasing Size Distributions for One-Dimensional Ga Rows on Si(100). *Phys. Rev. B* **2005**, *72*, 035426.
27. Kocán, P.; Sobotík, P.; Ošťádal, I.; Javorský, J.; Setvín, M. Stability of In Rows on Si(100) During STM Observation. *Surf. Sci.* **2007**, *601*, 4506–4509.
28. Saranin, A. A.; Zotov, A. V.; Kuyanov, I. A.; Kotlyar, V. G.; Kishida, M.; Murata, Y.; Okado, H.; Matsuda, I.; Morikawa, H.; Miyata, N.; Hasegawa, S.; Katayama, M.; Oura, K. Long-period Modulation in the Linear Chains of Tl Atoms on Si(100). *Phys. Rev. B* **2005**, *71*, 165307.
29. Glueckstein, J. G.; Evans, M. M. R.; Nogami, J. Growth of Sn on Si(001) at Room Temperature. *Surf. Sci.* **1998**, *415*, 80–94.
30. Dong, Z.-C.; Fujita, D.; Nejoh, H. Adsorption and Tunneling of Atomic Scale Lines of Indium and Lead on Si(100). *Phys. Rev. B* **2001**, *63*, 115402.
31. Nolph, C. A.; Liu, H.; Reinke, P. Bonding Geometry of Mn-Wires on the Si(100)(2 × 1) Surface. *Surf. Sci.* **2011**, *605*, L29–L32.
32. Owen, J. H. G.; Miki, K.; Koh, H.; Yeom, H. W.; Bowler, D. R. Stress Relief as the Driving Force for Self-Assembled Bi Nanolines. *Phys. Rev. Lett.* **2002**, *88*, 226104.
33. Walsh, M. A.; Walter, S. R.; Bevan, K. H.; Geiger, F. M.; Hersam, M. C. Phenylacetylene One-Dimensional Nanostructures on the Si(100)-2 × 1:H Surface. *J. Am. Chem. Soc.* **2010**, *132*, 3013–3019.
34. Giessibl, F. J. Advances in Atomic Force Microscopy. *Rev. Mod. Phys.* **2003**, *75*, 949–983.
35. Sader, J. E.; Jarvis, S. P. Accurate Formulas for Interaction Force and Energy in Frequency Modulation Force Spectroscopy. *Appl. Phys. Lett.* **2004**, *84*, 1801–1803.
36. Sugimoto, Y.; Pou, P.; Custance, O.; Jelinek, P.; Morita, S.; Perez, R.; Abe, M. Real Topography, Atomic Relaxations, and Short-range Chemical Interactions in Atomic Force Microscopy: The Case of the α-Sn/Si(111)-($\sqrt{3} \times \sqrt{3}$)R30° Surface. *Phys. Rev. B* **2006**, *73*, 205329.
37. Li, Y. J.; Nomura, H.; Ozaki, N.; Naitoh, Y.; Kageshima, M.; Sugawara, Y.; Hobbs, C.; Kantorovich, L. Origin of p(2 × 1) Phase on Si(001) by Noncontact Atomic Force Microscopy at 5 K. *Phys. Rev. Lett.* **2006**, *96*, 106104.
38. Oyabu, N.; Pou, P.; Sugimoto, Y.; Jelinek, P.; Abe, M.; Morita, S.; Perez, R.; Custance, O. Single Atomic Contact Adhesion and Dissipation in Dynamic Force Microscopy. *Phys. Rev. Lett.* **2006**, *96*, 106101.
39. Majzik, Z.; Setvín, M.; Bettac, A.; Feltz, A.; Cháb, V.; Jelínek, P. Simultaneous Current, Force and Dissipation Measurements on the Si(111)-7 × 7 Surface with an Optimized qPlus AFM/STM Technique. *Beilstein J. Nanotechnol.* **2012**, *3*, 249–259.
40. Weymouth, A. J.; Wutscher, T.; Welker, J.; Hofmann, T.; Giessibl, F. J. Phantom Force Induced by Tunneling Current: A Characterization of Si(111). *Phys. Rev. Lett.* **2011**, *106*, 226801.
41. Hata, K.; Kimura, T.; Ozawa, S.; Shigekawa, H. How to Fabricate a Defect Free Si(001) Surface. *J. Vac. Sci. Technol. A* **2000**, *18*, 1933–1936.
42. Lewis, J. P.; Glaesemann, K. R.; G. A. Voth, J. F.; Demkov, A. A.; Ortega, J.; Sankey, O. F. Further Developments in the Local-orbital Density-Functional-Theory Tight-binding Method. *Phys. Rev. B* **2001**, *64*, 195103.
43. Jelinek, P.; Wang, H.; Lewis, J.; Sankey, O. F.; Ortega, J. Multicenter Approach to the Exchange-Correlation Interactions in *ab Initio* Tight-Binding Methods. *Phys. Rev. B* **2005**, *71*, 235101.
44. Pou, P.; Ghasemi, S. A.; Jelinek, P.; Lenosky, T.; Goedecker, S.; Perez, R. Structure and Stability of Semiconductor Tip Apexes for Atomic Force Microscopy. *Nanotechnology* **2009**, *20*, 264015.